



Wave propagation in grains, soils, and rocks, modelled as an elastic reduced Cosserat continuum

Elena F. Grekova  (elgreco@pdmi.ras.ru),
G rard C. Herman  (gerard.herman@shell.com)

 Institute for Problems in Mechanical Engineering
of Russian Academy of Sciences, St. Petersburg, Russia

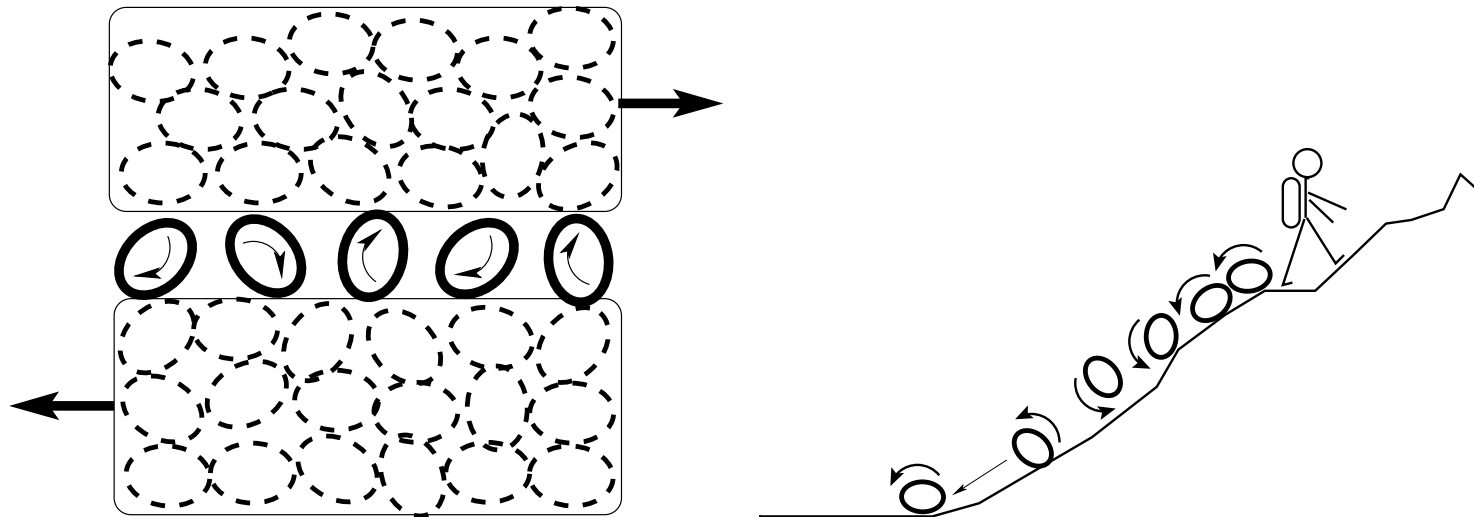
 Shell E. & P., Rijswijk, the Netherlands

This research was supported by Shell International E.& P. (Project “Waves in complex media”).

Many thanks to the organisers of the “Granular session” at the Institut Henri Poincaré for their kind invitation.

Motivation

Rotational degrees of freedom of particles in granular materials may be important for modelling of shear processes, avalanches, investigation of stability of granular systems, flowability.



Experimental evidences: A. Corfdir, P. Lerat, and J.-N. Roux. Translation and rotation of grains within an interface between granular media and structure. PG2001.

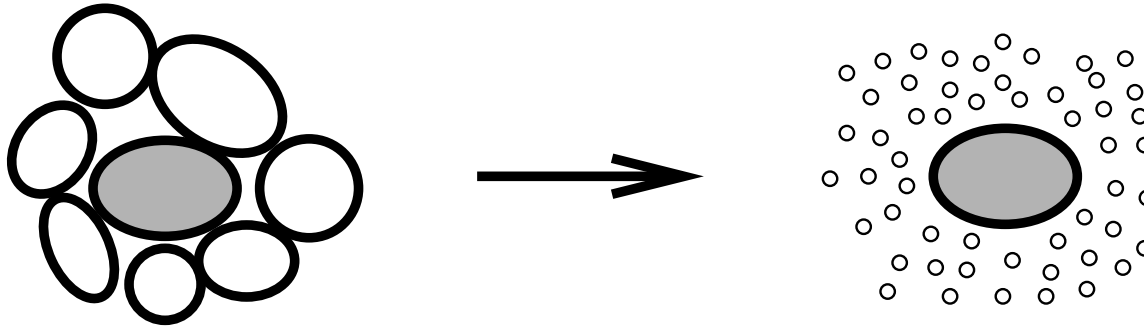
Theoretical and numerical considerations:

L.M. Schwartz, D.L. Johnson, S. Feng (1984, reduced Cosserat continuum).

Cosserat continuum: I. Vardoulakis and P. Unterreiner (1995); R. de Borst, A. Suiker, ...

In soils (highly compressed granular materials) and rocks there are heterogeneities, which may have their proper rotational dynamics in certain range of frequencies that influences wave propagation

Effective model for granular materials

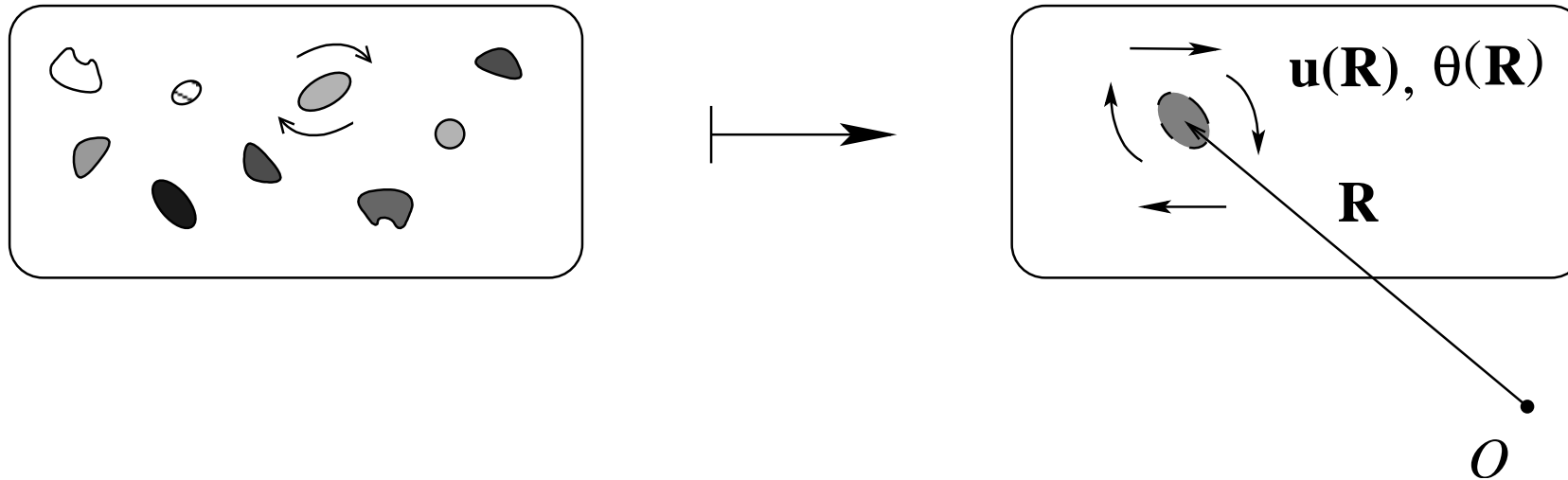


We introduce a set of interacting quasi-grains that can mimic the behaviour of a real granular material.

Background medium resists to the rotation and translation of each point-body. There is no “rotational spring” keeping rotations of neighbouring grains close \implies the stress tensor is not symmetric, but the couple stress is zero (reduced Cosserat continuum).

Effective model (rocks)

Rock is a complex material with such wave properties as **attenuation and dispersion**, caused by its microstructure.



classical heterogeneous medium with cracks, pores, inclusions, layers

enriched homogeneous medium — reduced Cosserat continuum with anisotropy

classical wave equation with inhomogeneous moduli scattering problems

complex wave equation with homogeneous moduli

Equations for the reduced Cosserat continuum

$\mathbf{g} = \nabla \mathbf{u} + \boldsymbol{\theta} \times \mathbf{E}$ — tensor of deformation

The deformation energy of the medium

$$U = \frac{1}{2}(\mathbf{g}^S \cdot \cdot \mathbf{C} \cdot \cdot \mathbf{g}^S + \mathbf{g}^A \cdot \cdot \mathbf{Z} \cdot \cdot \mathbf{g}^A + \varepsilon \mathbf{g}^S \cdot \cdot \mathbf{N}_{(a)} \cdot \cdot \mathbf{g}^A + \varepsilon \mathbf{g}^A \cdot \cdot \mathbf{N}_{(s)} \cdot \cdot \mathbf{g}^S)$$

Constitutive equation:

$$\boldsymbol{\tau} = \mathbf{C} \cdot \cdot \mathbf{g}^S + \mathbf{Z} \cdot \cdot \mathbf{g}^A + \varepsilon(\mathbf{N}_{(a)} + \mathbf{N}_{(s)}) \cdot \cdot \mathbf{g}$$

If $\mathbf{N}_{(a)} = \mathbf{N}_{(s)} = \mathbf{0}$ (isotropic case), there is no coupling between shear and compression wave. Weak anisotropy: $\varepsilon = o(1)$,

$$\mathbf{C} = \lambda \mathbf{E} \mathbf{E} + 2\mu (\mathbf{i}_m \mathbf{i}_n)^S (\mathbf{i}^n \mathbf{i}^m)^S, \quad \mathbf{Z} = 2\alpha (\mathbf{i}_m \mathbf{i}_n)^A (\mathbf{i}^m \mathbf{i}^n)^A,$$

$$\boldsymbol{\tau} = \boldsymbol{\tau}^{\text{classical}} + \boldsymbol{\tau}^\alpha + \varepsilon \mathbf{N} \cdot \cdot \mathbf{g}, \quad (1)$$

$\boldsymbol{\tau}^{\text{classical}} = \lambda \mathbf{E} \nabla \cdot \mathbf{u} + 2\mu (\nabla \mathbf{u})^S$ is the classical elastic stress tensor,

$$\boldsymbol{\tau}^\alpha = 2\alpha (\nabla \mathbf{u} + \boldsymbol{\theta} \times \mathbf{E})^A, \quad \mathbf{N} = \mathbf{N}_{(a)} + \mathbf{N}_{(s)}.$$

Balance of force and the balance of torque:

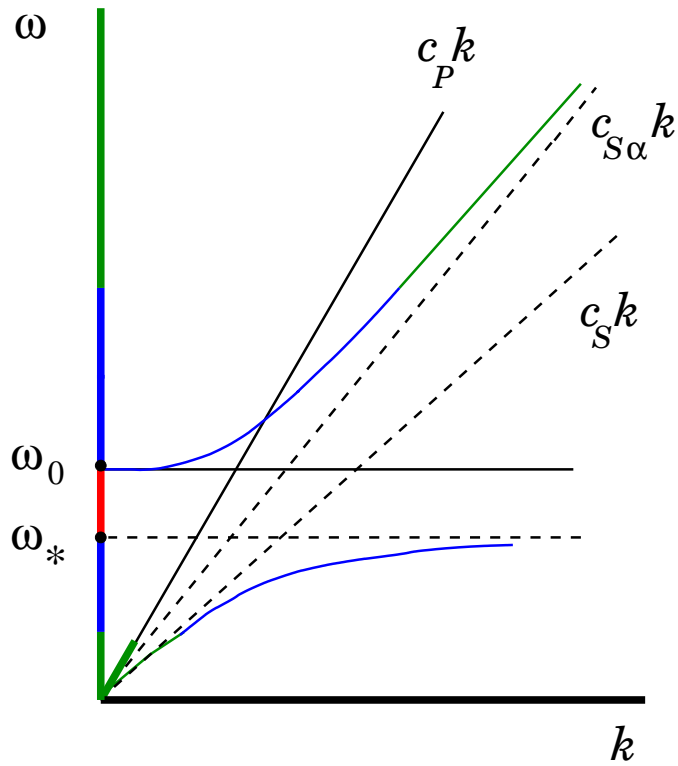
$$\nabla \cdot \boldsymbol{\tau} + \rho \mathbf{K} = \rho \ddot{\mathbf{u}}, \quad \boldsymbol{\tau}_{\times} + \rho \mathbf{L} = (\mathbf{I} \cdot \dot{\boldsymbol{\theta}}).$$

Equation of motion in displacements for zero external loads:

$$\begin{aligned} (\lambda + \mu) \nabla \nabla \cdot \mathbf{u} - \mu \Delta \mathbf{u} + \varepsilon \nabla \cdot (\mathbf{N}_{(a)} \cdot \cdot (\boldsymbol{\theta} \times \mathbf{E} + (\nabla \mathbf{u})^A) \\ = \rho (\ddot{\mathbf{u}} + \nabla \times (\mathbf{I} \cdot \ddot{\boldsymbol{\theta}} / 2)) \\ 2\alpha \nabla \times \mathbf{u} + \varepsilon (\mathbf{N}_{(s)} \cdot \cdot (\nabla \mathbf{u})^S)_{\times} - 4\alpha \boldsymbol{\theta} = \mathbf{I} \cdot \ddot{\boldsymbol{\theta}} \end{aligned}$$

We shall consider a spheric inertia tensor: $\mathbf{I} = I \mathbf{E}$ (for simplicity).

Plane waves for the isotropic case ($\varepsilon = 0$):



Dispersion curves. The P wave is not affected; the S wave is strongly frequency dependent and has a “forbidden zone” for $\omega_* < \omega < \omega_0$, where the wave decays exponentially with depth. The horizontal line corresponds to the non-propagating rotational oscillations of point bodies. $c_P^2 = (\lambda + 2\mu)/\rho$, $c_{S\alpha}^2 = (\mu + \alpha)/\rho$, $c_S^2 = \mu/\rho$, $\omega_0^2 = 4\alpha/I$, $\omega_*^2 = \omega_0^2/(1 + \alpha/\mu)$.

Shear dispersion relation:

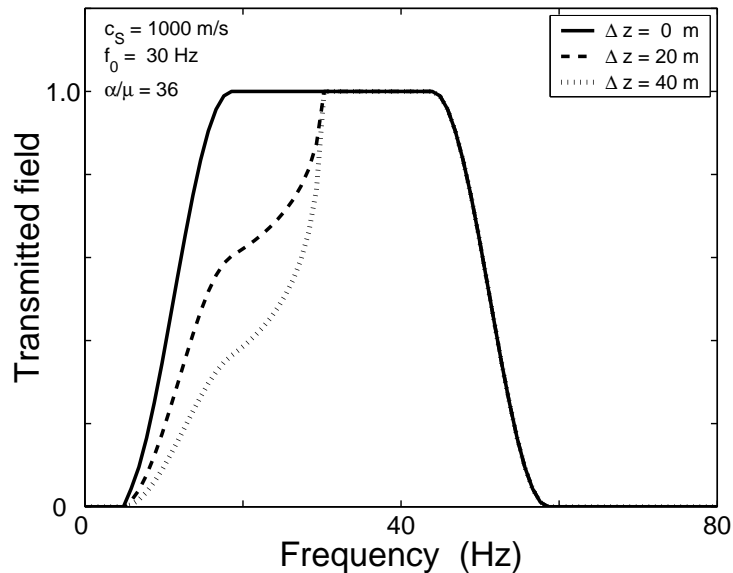
$$k_S^2 = \frac{\omega^2}{c_S^2} \cdot \frac{1 - \omega^2/\omega_0^2}{1 - \omega^2/\omega_*^2} = \frac{\omega^2}{c_S^2} f^2(\omega).$$

Eigenvectors:

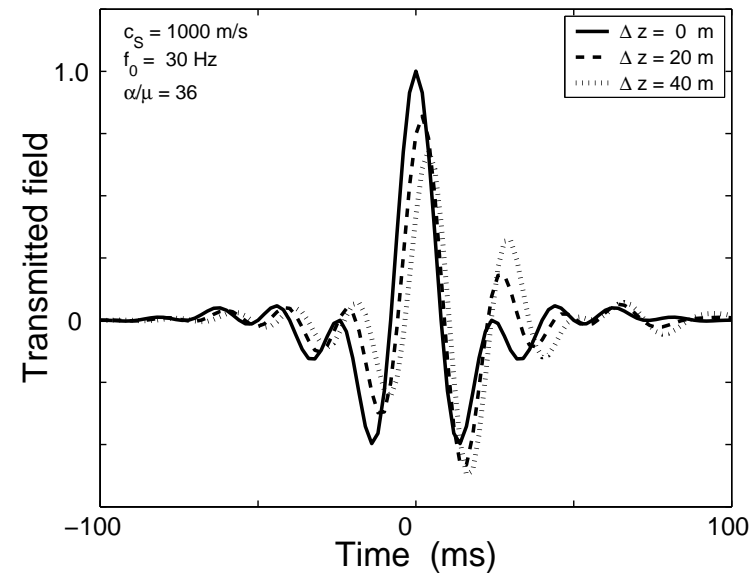
$$\begin{aligned} \mathbf{u} = & 4\alpha(-((\lambda + \mu - \alpha)(1 - \omega^2/\omega_0^2) + \alpha)\mathbf{k}_1\mathbf{k}_1 \cdot \mathbf{A}_1 e^{i(\mathbf{k}_1 \cdot \mathbf{r} - \omega t)} + \\ & ((\lambda + 2\mu)(1 - \omega^2/\omega_0^2)(k_s^2 - \omega^2/c_P^2)\mathbf{a}_1 - \\ & - ((\lambda + \mu - \alpha)(1 - \omega^2/\omega_0^2) + \alpha)\mathbf{k}_s\mathbf{k}_s \cdot \mathbf{a}_1 + \\ & i2\alpha(1 - \omega^2/\omega_0^2)\mathbf{k}_s \times \mathbf{a}_2) e^{i(\mathbf{k}_s \cdot \mathbf{r} - \omega t)} \end{aligned}$$

$$\begin{aligned} \theta = & \nabla \nabla \cdot \mathbf{A}_2(\mathbf{r}) e^{i\omega_0 t} + \\ & e^{i(\mathbf{k}_s \cdot \mathbf{r} - \omega t)} 2\alpha(2(\mu + \alpha)(1 - \omega^2/\omega_0^2)(k_s^2 - \omega^2/c_{S\alpha}^2)\mathbf{a}_2 - \\ & 2\alpha\mathbf{k}_s\mathbf{k}_s \cdot \mathbf{a}_2 + (\lambda + 2\mu)(k_s^2 - \omega^2/c_P^2)\mathbf{k}_s \times \mathbf{a}_1) \end{aligned}$$

How do the wave forms look like?

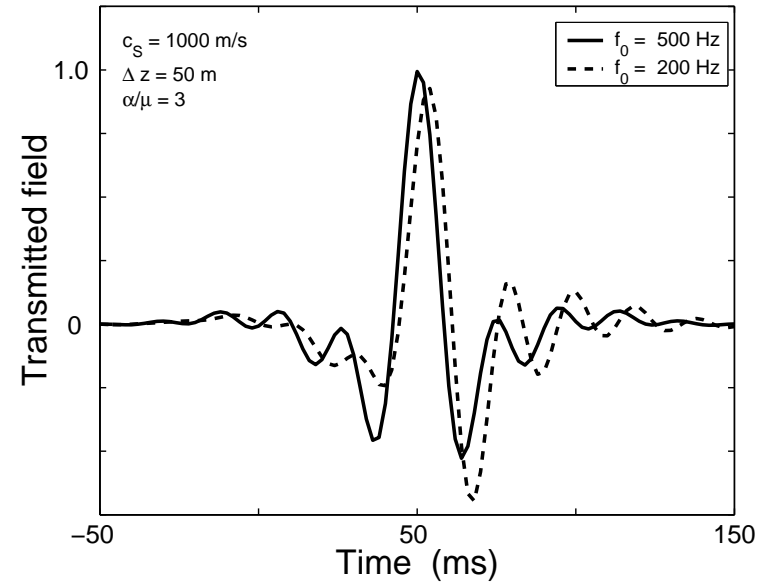
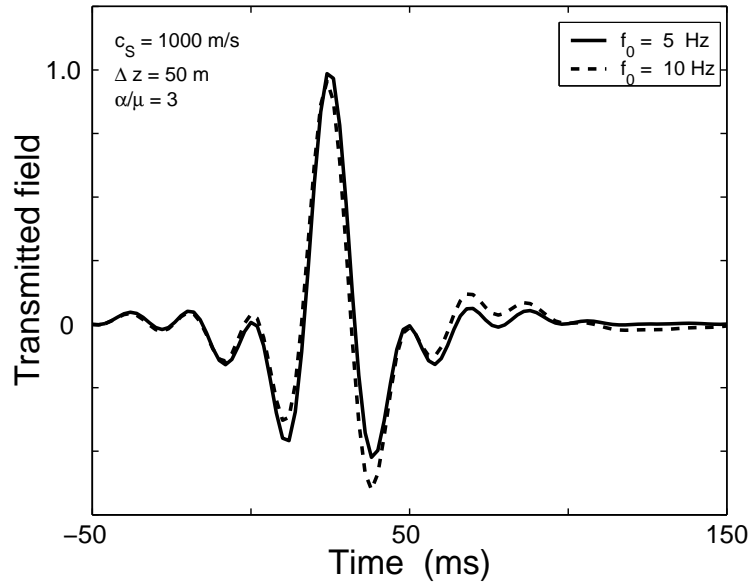


(a) Frequency domain



(b) Time domain

Transmitted shear wave for various propagation distances Δz when the seismic frequency range overlaps the “forbidden” zone $\omega_* < \omega < \omega_0$ ($f_0 = \omega_0/2\pi$). Strong attenuation and dispersion are observed, even for small values of Δz .



Similar to figure 3, but now for the cases when the seismic frequency range is either higher (a) or lower (b) than the frequency range of the **forbidden zone**.

Green functions ($\rho\mathbf{K} = \mathbf{K}_0 e^{i\omega t} \delta(\mathbf{r})$, $\rho\mathbf{L} = \mathbf{L}_0 e^{i\omega t} \delta(\mathbf{r})$):

Localization phenomena at $\omega_* \leq \omega < \omega_0$:

$$\mathbf{u} = \frac{\mathbf{K}_0 e^{i\omega t}}{4\pi\mu(\lambda + 2\mu)} \left(\frac{\omega^2}{c_P^2} + |k_s|^2 \right)^{-1} \left(\frac{\omega^2}{\omega_*^2} - 1 \right)^{-1} \cdot \left(- e^{-i\frac{\omega}{c_P} r} (\dots) + \right. \\ \left. e^{-|k_s| r} \left(\frac{1}{r} \mathbf{E} \left(1 - \frac{\omega^2}{\omega_0^2} \right) (\lambda + 2\mu) \left(\frac{\omega^2}{c_P^2} + |k_s|^2 \right) \right. \right. \\ \left. \left. + \left((\lambda + \mu - \alpha) \left(1 - \frac{\omega^2}{\omega_0^2} \right) + \alpha \right) \left(-\frac{1}{r} |k_s|^2 \hat{\mathbf{r}} \hat{\mathbf{r}} + (1 + |k_s| r) \frac{\mathbf{E} - 3\hat{\mathbf{r}} \hat{\mathbf{r}}}{r^3} \right) \right) \right) \\ + \frac{\mathbf{L}_0 e^{i\omega t}}{8\pi\alpha\mu} \left(1 - \frac{\omega^2}{\omega_*^2} \right)^{-1} \cdot \frac{\mathbf{E} \times \hat{\mathbf{r}}}{r^2} (1 + |k_s| r) e^{-|k_s| r}$$

at ω_0 if $\mathbf{L}_0 = \mathbf{0}$

$$\mathbf{u} = -\frac{\mathbf{K}_0 e^{i\omega_0 t}}{4\pi\rho\omega_0^2} \cdot \left(\frac{\mathbf{E} - 3\hat{\mathbf{r}} \hat{\mathbf{r}}}{r^3} - e^{-i\frac{\omega_0}{c_P} r} \left(\frac{1}{r} \frac{\omega_0^2}{c_P^2} \hat{\mathbf{r}} \hat{\mathbf{r}} + \left(1 + i\frac{\omega_0}{c_P} r \right) \frac{\mathbf{E} - \hat{\mathbf{r}} \hat{\mathbf{r}}}{r^3} \right) \right)$$

$$\boldsymbol{\theta} = e^{i\omega t} e^{-|k_s|r} \left(\frac{\omega^2}{\omega_*^2} - 1 \right)^{-1} \left(\frac{\mathbf{L}_0}{16\pi\alpha^2\mu} \left(1 - \frac{\omega^2}{\omega_0^2} \right)^{-1} \right.$$

$$\left. \left(\frac{1}{r} \mathbf{E} \left(1 - \frac{\omega^2}{\omega_0^2} \right) \left(\frac{\omega^2}{c_{s\alpha}^2} + |k_s|^2 \right) (\mu + \alpha) - \frac{\hat{\mathbf{r}}\hat{\mathbf{r}}}{r} |k_s|^2 \alpha + \frac{\mathbf{E} - 3\hat{\mathbf{r}}\hat{\mathbf{r}}}{r^3} (1 + |k_s|r) \alpha \right) \right.$$

$$\left. + \frac{\mathbf{K}_0}{8\pi\mu} \cdot \frac{\mathbf{E} \times \hat{\mathbf{r}}}{r^2} (1 + |k_s|r) \right)$$

Weak anisotropy

Anisotropic coupling leads to the similar frequency-dependent phenomena for the P-wave.

Plane wave propagation: $\mathbf{u} = \mathbf{U}e^{i(\mathbf{k}\cdot\mathbf{r}-\omega t)}$, $\boldsymbol{\theta} = \boldsymbol{\Theta}e^{i(\mathbf{k}\cdot\mathbf{r}-\omega t)}$.

$$-(\lambda + \mu)\mathbf{k}\mathbf{k} \cdot \mathbf{U} + (-\mu k^2 + \rho\omega^2)\mathbf{U} + iI\omega^2\mathbf{k} \times \boldsymbol{\Theta}/2 \\ + \varepsilon i\mathbf{k} \cdot (\mathbf{N}_{(a)} \cdot \cdot (\boldsymbol{\Theta} \times \mathbf{E} + i(\mathbf{k}\mathbf{U})^A) = \mathbf{0}$$

$$(4\alpha - I\omega^2)\boldsymbol{\Theta} = 2i\alpha\mathbf{k} \times \mathbf{U} + \varepsilon i(\mathbf{E} \times \mathbf{E}) \cdot \cdot (\mathbf{N}_{(s)} \cdot \cdot (\mathbf{k}\mathbf{U})^S)$$

(A) $4\alpha - I\omega^2 = O(1)$. Up to the higher order terms

$$\boldsymbol{\Theta} = i(4\alpha - I\omega^2)^{-1}(2\alpha\mathbf{k} \times \mathbf{U} + \varepsilon(\mathbf{E} \times \mathbf{E}) \cdot \cdot (\mathbf{N}_{(s)} \cdot \cdot (\mathbf{k}\mathbf{U})^S))$$

$$\left[(\rho\omega^2 - (\lambda + 2\mu)k^2)\hat{\mathbf{k}}\hat{\mathbf{k}} + (\rho\omega^2 - (\mu + \alpha\frac{\omega^2}{\omega^2 - \omega_0^2})k^2)(\mathbf{E} - \hat{\mathbf{k}}\hat{\mathbf{k}}) \right.$$

$$\left. - \varepsilon\frac{\omega^2 k^2}{\omega^2 - \omega_0^2}\hat{\mathbf{k}} \cdot \mathbf{N} \cdot \hat{\mathbf{k}} \right] \cdot \mathbf{U} = \mathbf{0}$$

The equation for the eigenvalues:

$$f_p(\omega, k) f_s^2(\omega, k) - \varepsilon^2 \frac{\omega^4 k^4}{(\omega^2 - \omega_0^2)^2} (\xi_{23}^2 f_p(\omega, k) + (\xi_{12}^2 + \xi_{13}^2) f_s(\omega, k)) = 0,$$

$$f_p(\omega, k) = \rho\omega^2 - (\lambda + 2\mu)k^2,$$

$$f_s(\omega, k) = \rho\omega^2 - \left(\mu + \frac{\alpha\omega^2}{(\omega^2 - \omega_0^2)^2}\right)k^2$$

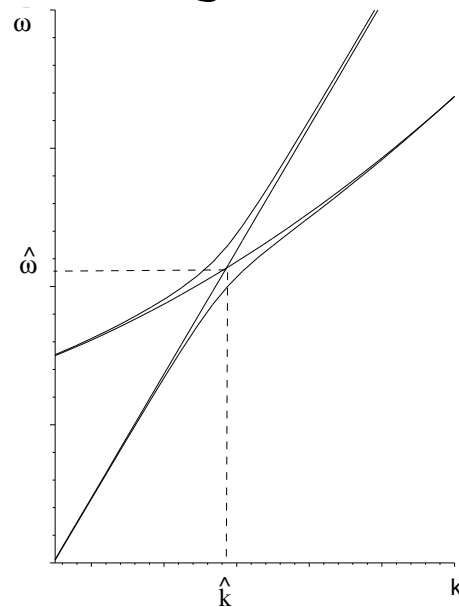
$$\mathbf{e}_1 = \hat{\mathbf{k}}, \quad \xi_{ij} = (\hat{\mathbf{k}} \cdot \mathbf{N} \cdot \hat{\mathbf{k}}) \cdots \mathbf{e}_i \mathbf{e}_j, \quad \mathbf{e}_i \cdot \mathbf{e}_j = \delta_{ij} \quad (2)$$

Far from the cross-point of dispersion curves for an isotropic medium $(\hat{\omega}, \hat{k})$ such that $f_p(\hat{\omega}, \hat{k}) = f_s(\hat{\omega}, \hat{k}) = 0$,

$\hat{\omega} = \sqrt{\frac{\alpha}{4(\lambda+\mu)}} + \sqrt{\frac{\alpha}{4(\lambda+\mu)} + \omega_0^2}$ the P-wave changes negligibly:

$$k = \frac{\omega}{c_p} + \frac{\varepsilon^2 \omega^5 (\xi_{12}^2 + \xi_{13}^2)}{2(\lambda + 2\mu) c_p^3 (\omega^2 - \omega_0^2) (\mu c_p^2 (c_s^2 - c_p^2) (\omega^2 - \omega_0^2) - \alpha \omega^2)}$$

Near the first cross-point (P-wave and shear-rotation wave)
the behaviour of the dispersion curves **changes qualitatively**:
coupling of compression and shear-rotation waves, a strong dis-
persion; the dispersion curves look like a hyperbola with asymp-
totes coinciding with tangents to the dispersion curves for an



isotropic medium.

The dispersion relation in the neighbourhood of the cross-point of partial curves is given by

$$\omega = \hat{\omega} + \tilde{\omega}, \quad k = \hat{k} + \tilde{k}, \quad (3)$$

$$(\tilde{\omega} - \tilde{k}(c_{g1} + c_{g2})/2)^2 - \tilde{k}(c_{g1} - c_{g2})^2/4 = b_*, \quad (4)$$

where $c_{g1} = c_p$, c_{g2} are group velocities of the dispersion curves for the case of isotropic medium in the cross-point, b_* is determined by ξ_{ij} and medium constants.

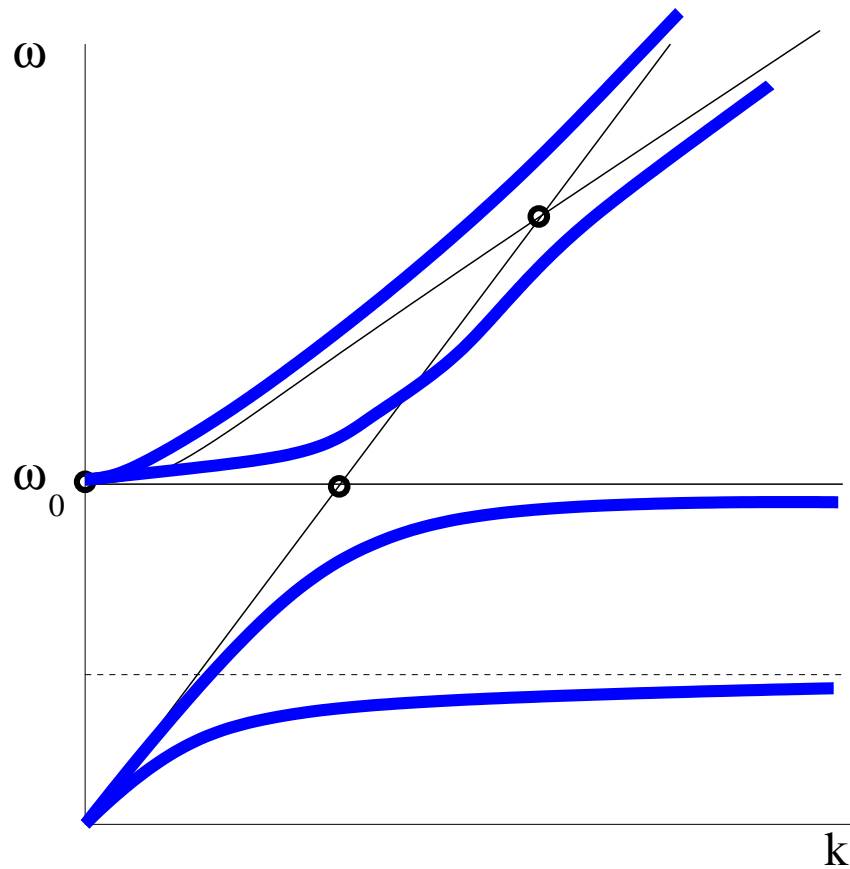
Second cross-point: $\omega = \omega_0$, $k = 0$ — shear-rotation curve and proper rotation line. We have to remake an asymptotic analysis, since

(B) $4\alpha - I\omega^2 = O(\varepsilon)$. The result:

$$\omega = \omega_0 + \varepsilon\tilde{\omega}, \quad k^2 = (\omega - \omega_0)\frac{2\rho\omega_0}{\alpha}$$

Third cross-point: $\hat{\omega} = \omega_0$, $\hat{k} = c_1^{-1}\omega_0$ — compression line and proper rotation line: in progress, but the result is similar to the one for the first-cross point. Again (B) $4\alpha - I\omega^2 = O(\varepsilon)$.

Even a weak anisotropy in elastic constants changes qualitatively plane wave propagation, causing the dispersive behaviour of the compression wave and its coupling with shear and rotation waves



Theoretical results

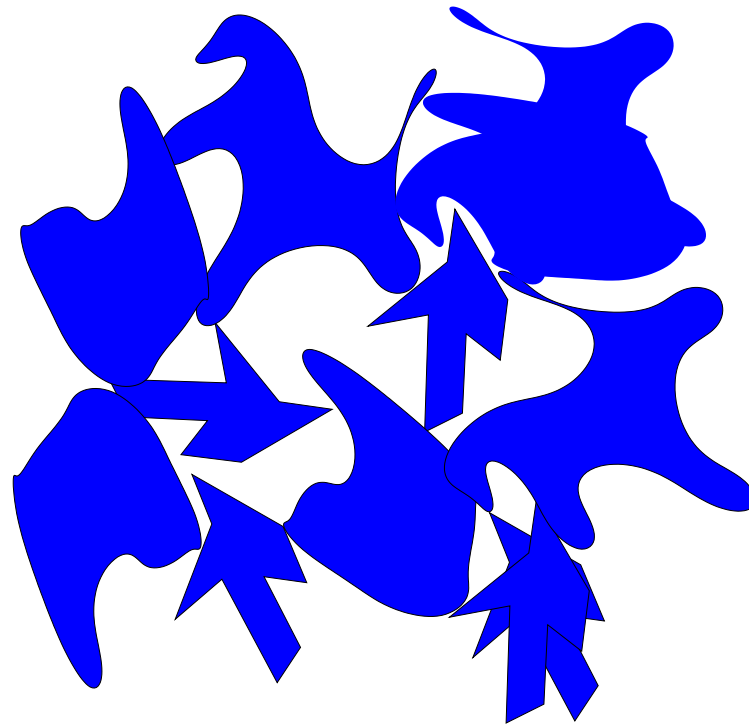
- The **reduced Cosserat theory** has been developed for modelling of the rock with inclusions possessing **proper rotational dynamics** (cracks, pores, heterogeneities), where the stress tensor is **asymmetric**.
- Plane wave solutions have been investigated. The **dispersive behaviour and attenuation**, similar to the ones observed in scattering problems, have been predicted for the **shear** wave propagation in a certain domain of frequencies. **Wave polarization** also appears in the model.
- Reaction of the system to a dynamic point source has been investigated, dynamic **Green functions** have been obtained. They change essentially their character depending on the source frequency. In a certain domain of frequency, **localization** phenomena are observed.
- Weak **anisotropy** coupling P- and S-waves, combined with rotational dynamics of medium particles, leads to similar effects for the P-wave

Robust conclusions for practical purposes (based on both models):

- there is a special frequency range where proper rotational dynamics of heterogeneities plays a role. This range is characterized by high dispersion, attenuation, and wave polarization
- there is a special frequency where we may expect very peculiar wave phenomena: localization, resonances, etc. The developed models **indicate**, but do not describe possible structural changes of a real medium subjected to the acoustical stimulation by (shear) wave at this frequency

Possible applications - ideas

- application of the developed theory for characterization of some soils, granular materials and fine powders: [rotational fluidization](#)



Plans

- To consider the **inhomogeneous** reduced Cosserat medium and to describe it in terms of an effective medium
- to make a good comparison with scattering problems
- to estimate medium constants via microstructural approach (in collaboration with S. Luding)
- laboratory experiments - verification of the model?

Appendix

Separated [equations of motion](#) (Sandru representation):

$$\square_1(\square_2\square_3 + 4\alpha^2\Delta)\Phi_1 = -\rho\mathbf{K},$$

$$\square_3(\square_2\square_3 + 4\alpha^2\Delta)\Phi_2 = -\rho\mathbf{L}.$$

$$\square_1 = (\lambda + 2\mu)(\Delta - c_P^{-2}\partial_t^2), \quad \square_2 = (\mu + \alpha)(\Delta - c_{S\alpha}^{-2}\partial_t^2), \quad \omega_0^2 = 4\alpha/I,$$
$$\square_3 = -4\alpha(1 + \omega_0^{-2}\partial_t^2),$$

Translational and angular displacements via Φ_1, Φ_2 :

$$\mathbf{u} = \square_1\square_3\Phi_1 - ((\lambda + \mu - \alpha)\square_3 - 4\alpha^2)\nabla\nabla \cdot \Phi_1 - 2\alpha\square_3\nabla \times \Phi_2$$

$$\boldsymbol{\theta} = \square_2\square_3\Phi_2 + 4\alpha^2\nabla\nabla \cdot \Phi_2 - 2\alpha\square_1\nabla \times \Phi_1$$

Green functions ($\rho\mathbf{K} = \mathbf{K}_0 e^{i\omega t} \delta(\mathbf{r})$, $\rho\mathbf{L} = \mathbf{L}_0 e^{i\omega t} \delta(\mathbf{r})$):

$$\Phi_1 = \mathbf{f}_0 e^{i\omega t} (e^{-i\omega r/c_P} - e^{-i\omega f(\omega)r/c_S})/r,$$

$$\Phi_2 = \mathbf{l}_0 e^{i\omega t} e^{-i\omega f(\omega)r/c_S}/r,$$

$$\begin{aligned} \mathbf{u} = & -\frac{\mathbf{K}_0 e^{i\omega t}}{4\pi\mu(\lambda + 2\mu)} \left(\frac{\omega^2}{c_P^2} - \frac{\omega^2 f^2(\omega)}{c_S^2} \right)^{-1} \left(1 - \frac{\omega^2}{\omega_*^2} \right)^{-1} \\ & \left(-e^{-i\frac{\omega}{c_P}r} \left((\lambda + \mu - \alpha) \left(1 - \frac{\omega^2}{\omega_0^2} \right) + \alpha \right) \left(\frac{1}{r} \frac{\omega^2}{c_P^2} \hat{\mathbf{r}}\hat{\mathbf{r}} + \left(1 + i\frac{\omega}{c_P}r \right) \frac{\mathbf{E} - 3\hat{\mathbf{r}}\hat{\mathbf{r}}}{r^3} \right) + \right. \\ & \left. e^{-i\frac{\omega f(\omega)}{c_S}r} \left(\frac{1}{r} \mathbf{E} \left(1 - \frac{\omega^2}{\omega_0^2} \right) (\lambda + 2\mu) \left(\frac{\omega^2}{c_P^2} - \frac{\omega^2 f^2(\omega)}{c_S^2} \right) \right. \right. \\ & \left. \left. + \left((\lambda + \mu - \alpha) \left(1 - \frac{\omega^2}{\omega_0^2} \right) + \alpha \right) \left(\frac{1}{r} \frac{\omega^2 f^2(\omega)}{c_S^2} \hat{\mathbf{r}}\hat{\mathbf{r}} + \left(1 + i\frac{\omega f(\omega)}{c_S}r \right) \frac{\mathbf{E} - 3\hat{\mathbf{r}}\hat{\mathbf{r}}}{r^3} \right) \right) \right) \\ & + \frac{\mathbf{L}_0 e^{i\omega t}}{8\pi\alpha\mu} \left(1 - \frac{\omega^2}{\omega_*^2} \right)^{-1} \cdot \frac{\mathbf{E} \times \hat{\mathbf{r}}}{r^2} \left(1 + i\frac{\omega f(\omega)}{c_S}r \right) e^{-i\frac{\omega f(\omega)}{c_S}r} \end{aligned}$$

$$\begin{aligned}
\boldsymbol{\theta} = & e^{i(\omega t - \frac{\omega f(\omega)}{c_S} r)} \left(1 - \frac{\omega^2}{\omega_*^2}\right)^{-1} \left(-\frac{\mathbf{L}_0}{16\pi\alpha^2\mu} \left(1 - \frac{\omega^2}{\omega_0^2}\right)^{-1} \right. \\
& \left. \left(\frac{1}{r} \mathbf{E} \left(1 - \frac{\omega^2}{\omega_0^2}\right) \left(\frac{\omega^2}{c_{S\alpha}^2} - \frac{\omega^2 f^2(\omega)}{c_S^2} \right) (\mu + \alpha) + \frac{1}{r} \hat{\mathbf{r}}\hat{\mathbf{r}} \frac{\omega^2 f^2(\omega)}{c_S^2} \alpha \right. \right. \\
& \left. \left. + \frac{1}{r^3} \left(1 + i \frac{\omega f(\omega)}{c_S} r\right) (\mathbf{E} - 3\hat{\mathbf{r}}\hat{\mathbf{r}}) \alpha \right) - \frac{\mathbf{K}_0}{8\pi\mu} \cdot \frac{\mathbf{E} \times \hat{\mathbf{r}}}{r^2} \left(1 + i \frac{\omega f(\omega)}{c_S} r\right) \right)
\end{aligned}$$